Supporting information

Direct dissolution of lignocellulosic biomass by malonic acid-DBU protonic ionic liquid and preparation of high-performance all-biomass films

Long Zhang[1], Boxiang Zhan [2], Shangzhong Zhang[3], Haiyuan Ji[4], Shen Peng[5], Minghui Fan[6], Lifeng Yan[7*]

[1,2,3,4,5,7]Key Laboratory of Precision and Intelligent Chemistry, and Department of Chemical Physics, University of Science and Technology of China, Jinzhai road, 230026, Hefei, Anhui, China.

[6]The Instruments Center for Physical Science, University of Science and Technology of China, Hefei, Jinzai Road 96, 230026 Anhui, China.

Number of pages-13, tables-5, figures-12

Supplementary Methods

1. Determination of cellulose, hemicellulose, and lignin content

The cellulose, hemicellulose, and lignin content in lignocellulose was determined according to improved National Renewable Energy Laboratory (NREL) procedures. 0.3 g of dry sample and 3 mL of 72 wt% sulphuric acid were added to a glass vial and stirred continuously for 1 hour. The mixture was then diluted to a concentration of 3 wt% sulphuric acid and heated at 121 °C for 1 hour. After cooling to room temperature, the liquid was filtered and injected into HPLC for analysis. The undissolved solid was filtered, washed, and dried to determine the lignin content. Glucose and xylose in cellulose and hemicellulose were determined by HPLC (SHIMADZU) with a refractive index detector (RID). Glucose and xylose were analyzed on an Inertsil amino column with a mobile phase of 70 wt% acetonitrile solution at a flow rate of 1 mL/min and a column temperature of 50 ℃. The yields of monosaccharides were calculated by calibrating the standard samples. Calculate the cellulose and hemicellulose content using glucose and xylose respectively. Lignin content was calculated using acid-insoluble lignin.

2. Determination of soluble substance content

Biomass powder and deionized water were mixed at a mass ratio of 1:25 and stirred continuously for 2 days at room temperature. The content of soluble substances in the biomass was calculated based on the weight difference.

3. Determination of wax content

The biomass was treated with toluene/ethanol (2: 1, v/v) through a Soxhlet extractor to remove wax. The content of wax in the biomass was calculated based on

the weight difference.

4. Determination of ash content

The biomass powder was placed in a tube furnace and heated at 700°C for 2 h. The content of ash in the biomass was calculated based on the weight difference.

Table S1. The composition of different biomass powders and the solubility in malonic acid-DBU PIL.

Type of biomass	Cellulose (%)	Hemicellulose (%)	Lignin (%)	Three constituents (%)	Soluble substance (%)	Wax (%)	Ash (%)	Other (%)	Solubility (wt%)
Corncob-1	29.31	31.24	16.90	77.45	11.62	3.65	2.04	5.24	10.2
Bamboo-1	31.04	21.57	27.87	80.48	7.74	2.11	5.40	4.27	8.4
Sorghum straw	25.23	22.25	22.23	69.71	17.38	2.63	7.68	4.60	7.5
Sugarcane bagasse	23.47	19.23	22.83	65.53	12.13	7.73	14.48	0.13	4.0
Plantago asiatica	21.30	18.42	21.37	61.09	12.20	1.40	20.96	4.35	3.4
Miscanthus giganteus	21.10	17.15	23.80	62.05	13.69	3.79	20.00	0.47	3.4
Poplar wood	25.23	12.38	19.03	56.64	9.32	6.22	21.86	5.96	2.7
Green grass	19.65	17.21	22.12	58.98	9.77	4.31	22.82	4.12	2.5
Pine wood	22.30	12.49	16.03	50.82	15.40	3.54	23.40	6.84	1.5
Rice husk	17.87	16.80	18.40	53.07	11.37	3.10	28.24	4.22	1.1
Corn straw	18.48	14.47	19.56	52.51	13.45	0.98	29.40	3.66	0.8

Note: The tests for component content and solubility of biomass powders were repeated three times under the same conditions.

Table S2. The composition of two corncobs and two bamboos and the solubility in malonic acid-DBU PIL.

Type of biomass	Cellulose (%)	Hemicellulose (%)	Lignin (%)	Soluble substance (%)	Wax (%)	Ash (%)	Other (%)	Solubility (wt%)
Corncob-1	29.31	31.24	16.90	11.62	3.65	2.04	5.24	10.2
Bamboo-1	31.04	21.57	27.87	7.74	2.11	5.40	4.27	8.4
Corncob-2	23.35	18.52	17.03	16.32	4.17	17.90	6.71	4.0
Bamboo-2	27.30	13.53	20.18	12.32	2.75	21.52	2.40	3.2

Note: The tests for component content and solubility of biomass powders were repeated three times under the same conditions.

Table S3. The composition of pure poplar wood and pure spruce wood and the solubility in malonic acid-DBU PIL.

Type of biomass	Cellulose (%)	Hemicellulose (%)	Lignin (%)	Three constituents (%)	Soluble substance (%)	Wax (%)	Ash (%)	Other (%)	Solubility (wt%)
Pure poplar wood	35.63	20.84	23.03	79.50	8.85	2.23	1.21	8.21	7.9
Pure spruce wood	43.17	18.18	22.60	83.95	5.12	1.68	1.01	8.24	8.2

Note: The tests for component content and solubility of biomass powders were repeated three times under the same conditions.

Table S4. The Kamlet-Taft (K-T) polarity parameters for malonic acid-DBU PILs and

other ILs.

Solvent systems	Kamlet-Taft parameters			References
	α	β	π*	
Malonic acid-DBU	0.94	1.39	0.70	This work[1]
[DBNH][Lev]	0.58	1.21	1.02	[2]
[DBUH][Lev]	0.49	1.20	1.04	[2]
EmimOAc/EA-DBN	0.51	1.12	1.00	[3]
PmimOAc/EA-DBN	0.56	1.10	0.96	[3]
BmimOAc/EA-DBN	0.63	1.01	1.04	[3]
AmimOAc/EA-DBN	0.63	0.99	1.04	[3]
EmimCl/EA-DBN	0.52	0.97	1.06	[3]
PmimCl/EA-DBN	0.57	0.97	1.06	[3]
BmimCl/EA-DBN	0.62	0.97	1.02	[3]
AmimCl/EA-DBN	0.68	0.94	1.02	[3]

Table S5. The ash content of different biomass films.

Biomass films	Corncob-4 wt%	Corncob-6 wt%	Corncob-8 wt%	Bamboo-4 wt%	Sorghum straw-4 wt%
Ash content	0.77%	0.72%	0.42%	3.44%	5.03%

Note: The tests for ash content were repeated three times under the same conditions.

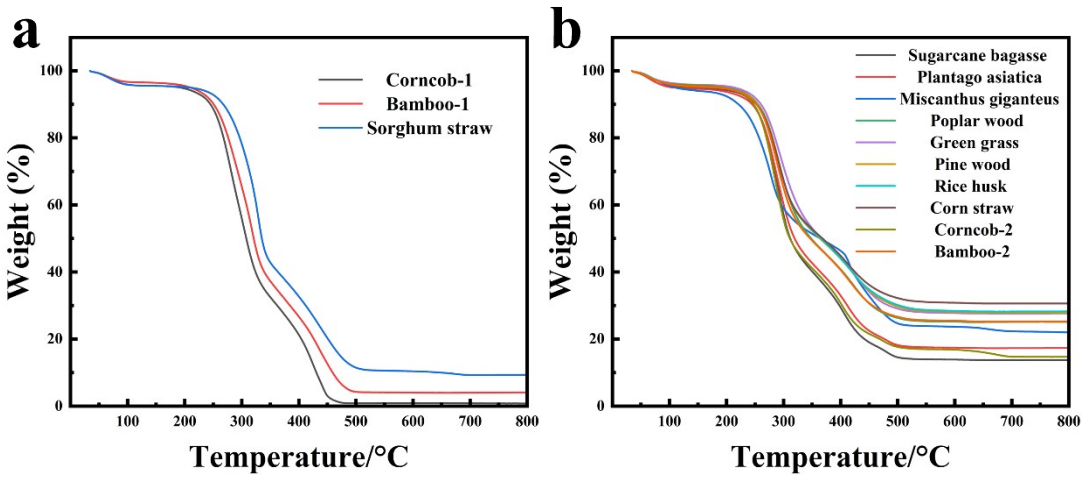

Figure S1. The TG curves of different biomasses in the air atmosphere.

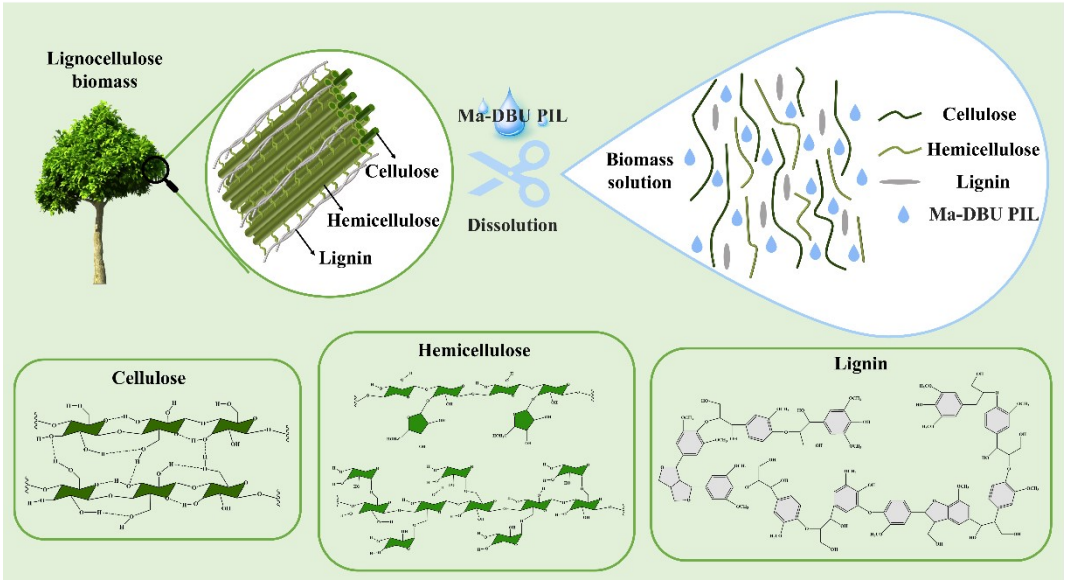

Figure S2. The dissolution process of lignocellulose and the molecular structures of cellulose, hemicellulose and lignin.

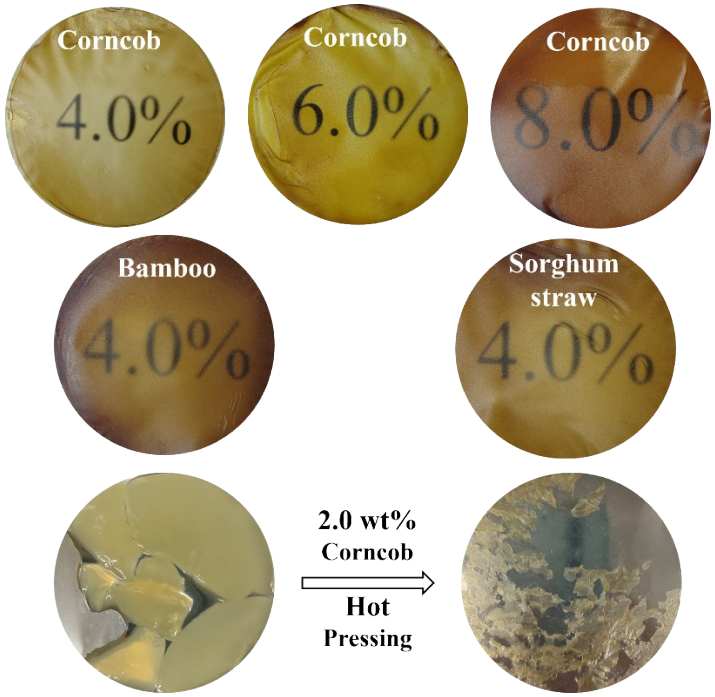

Figure S3. The photographs of different biomass films.

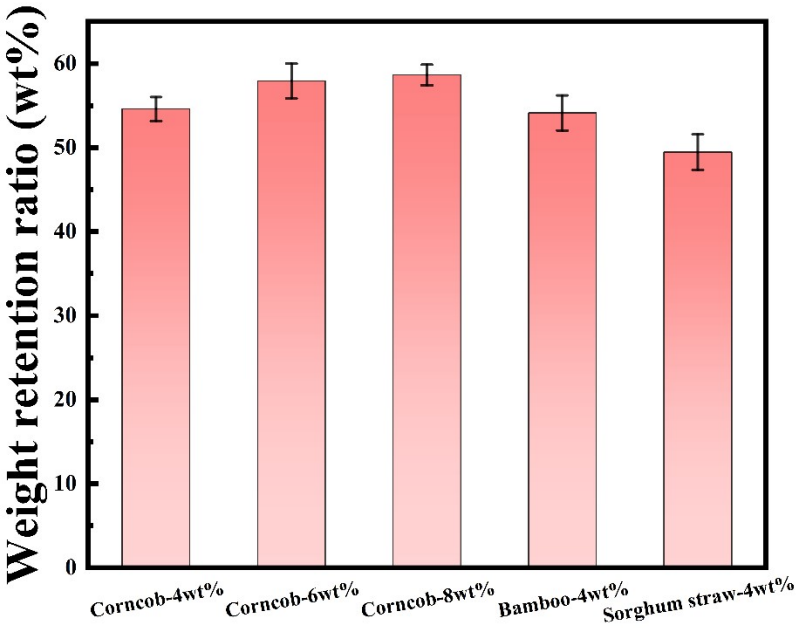

Figure S4. The weight retention ratios of different biomass films. (The tests were repeated three times under the same conditions)

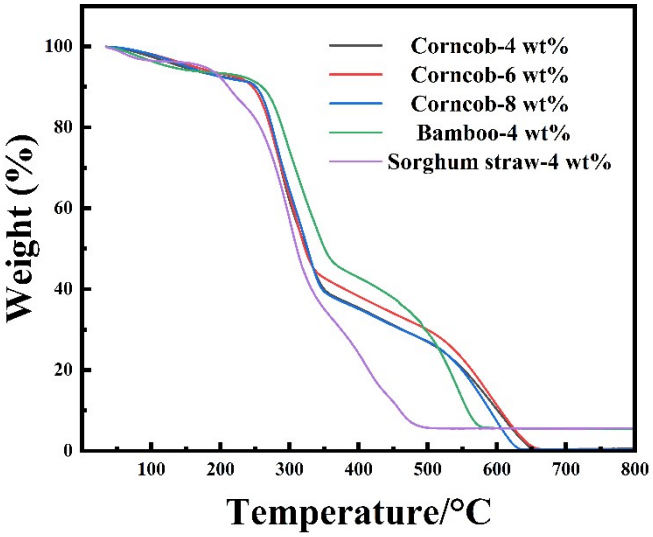

Figure S5. The TG curves of different biomass films in air atmosphere.

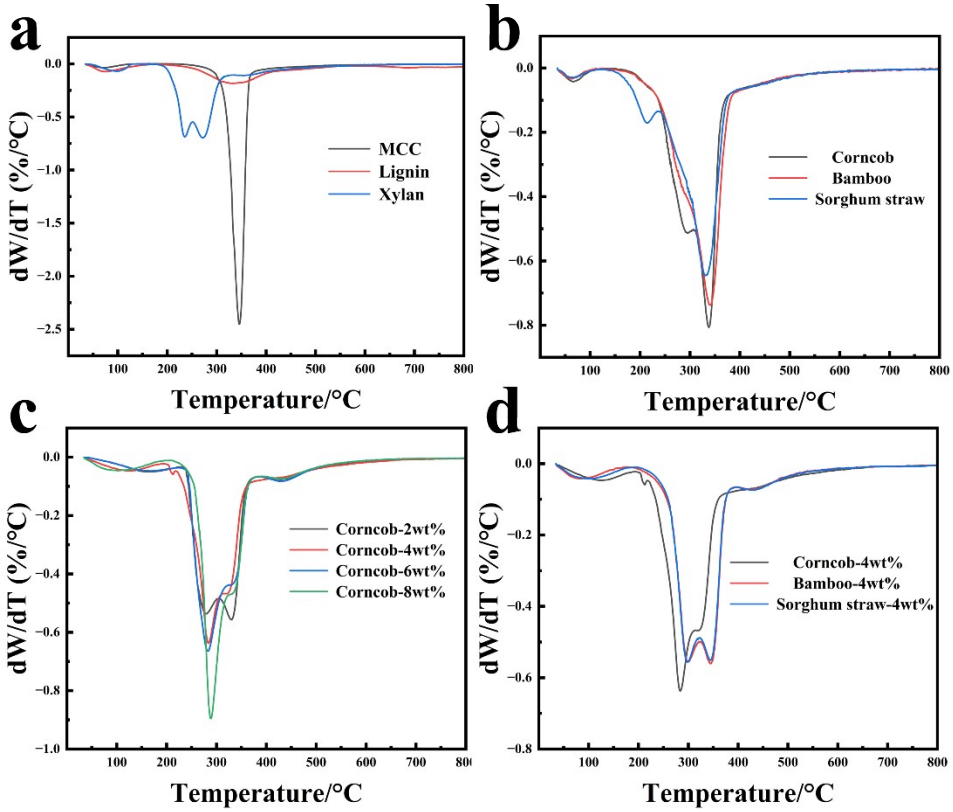

Figure S6. The DTG curves of cellulose, xylan, and lignin (a), corncob, bamboo, and sorghum straw (b), the corncob films with different concentrations (c), and different biomass films with the same concentration (d).

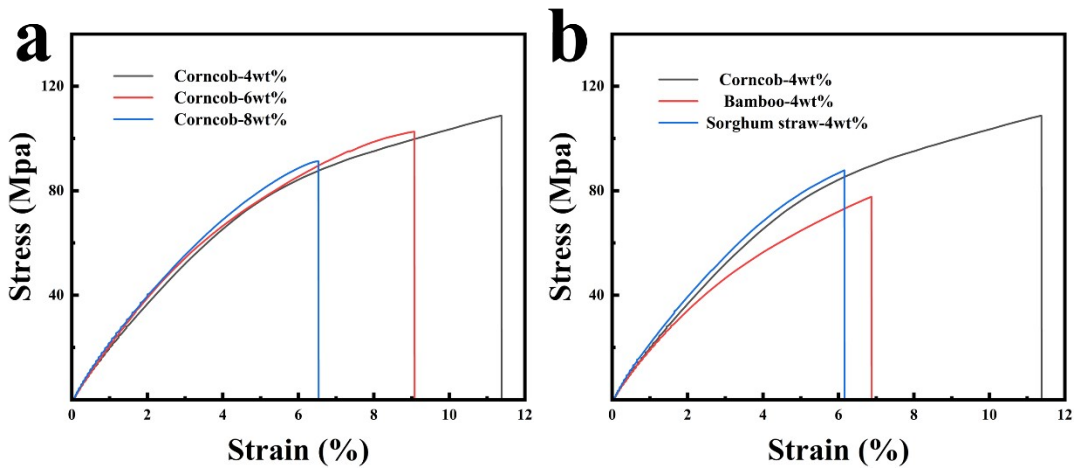

Figure S7. The stress-strain curves of the corncob films with different concentrations (a), and different biomass films with the same concentration (b).

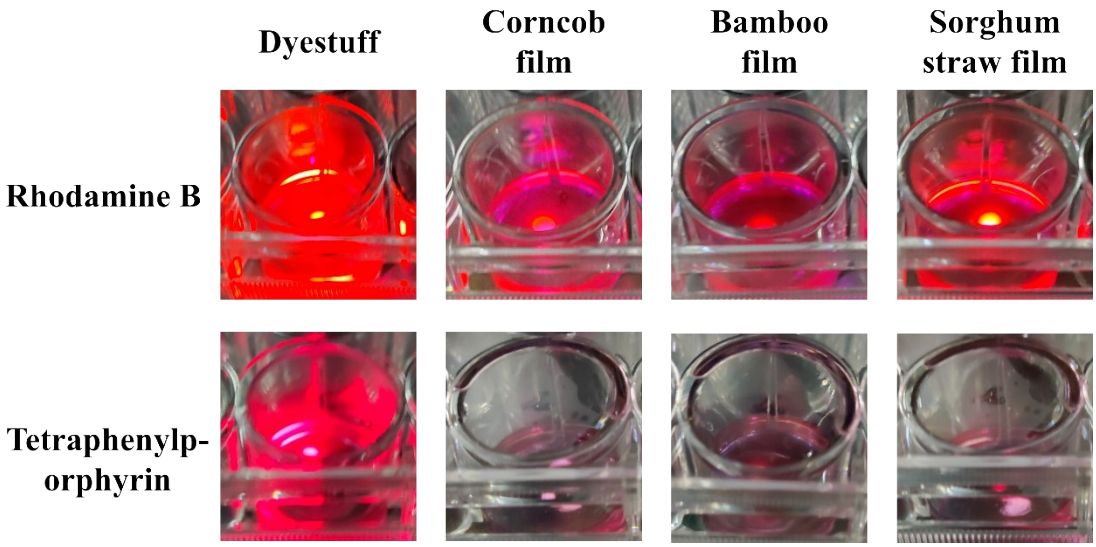

Figure S8. The macroscopic images of rhodamine B solution, tetraphenylporphyrin solution, and solutions covered by biomass films under the ultraviolet channel of an inverted fluorescence microscope.

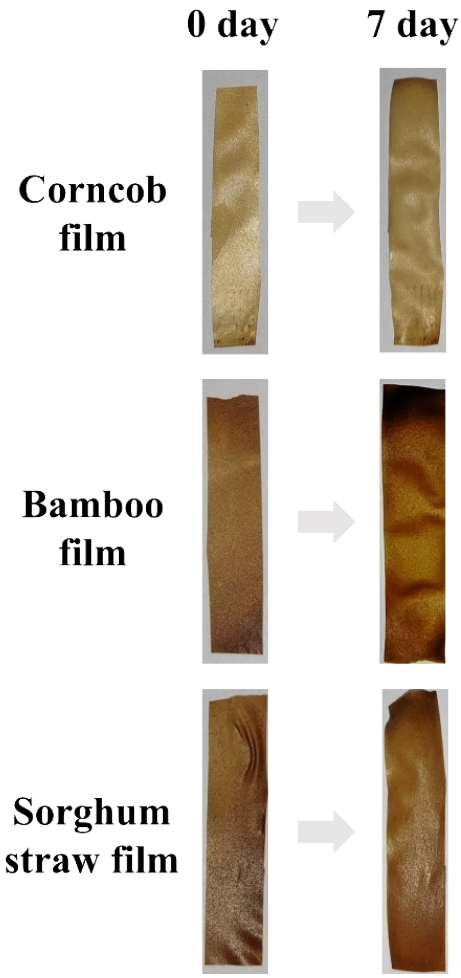

Figure S9. The images of different biomass films before and after 7 days of immersion in water.

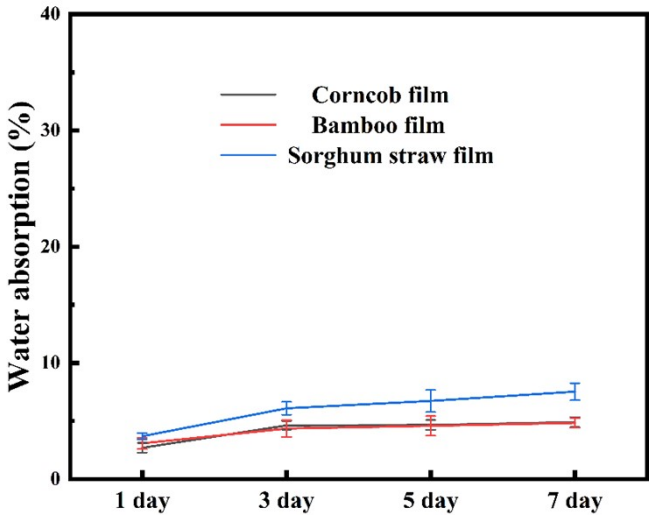

Figure S10. The water absorption of different biomass films. (The tests were repeated three times under the same conditions)

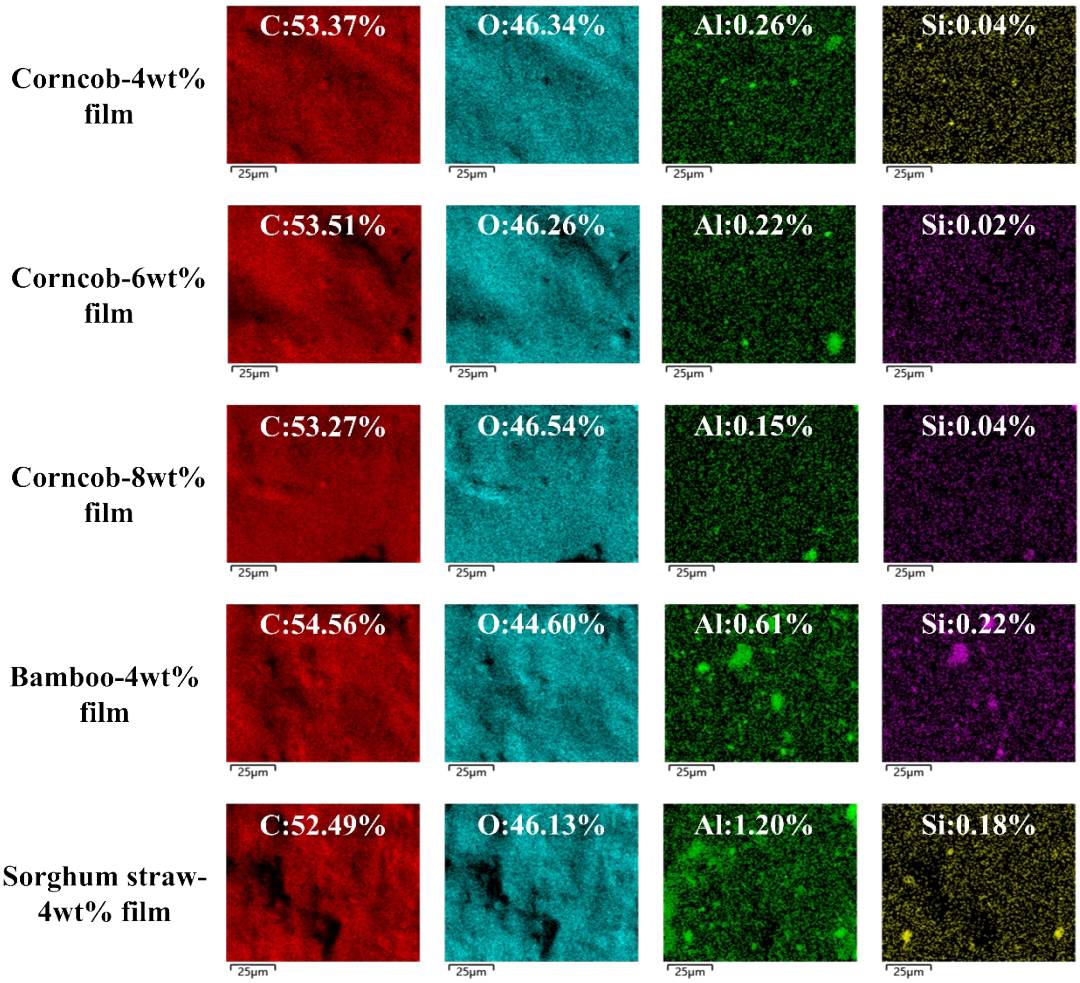

Figure S11. The elemental distribution of different biomass films.

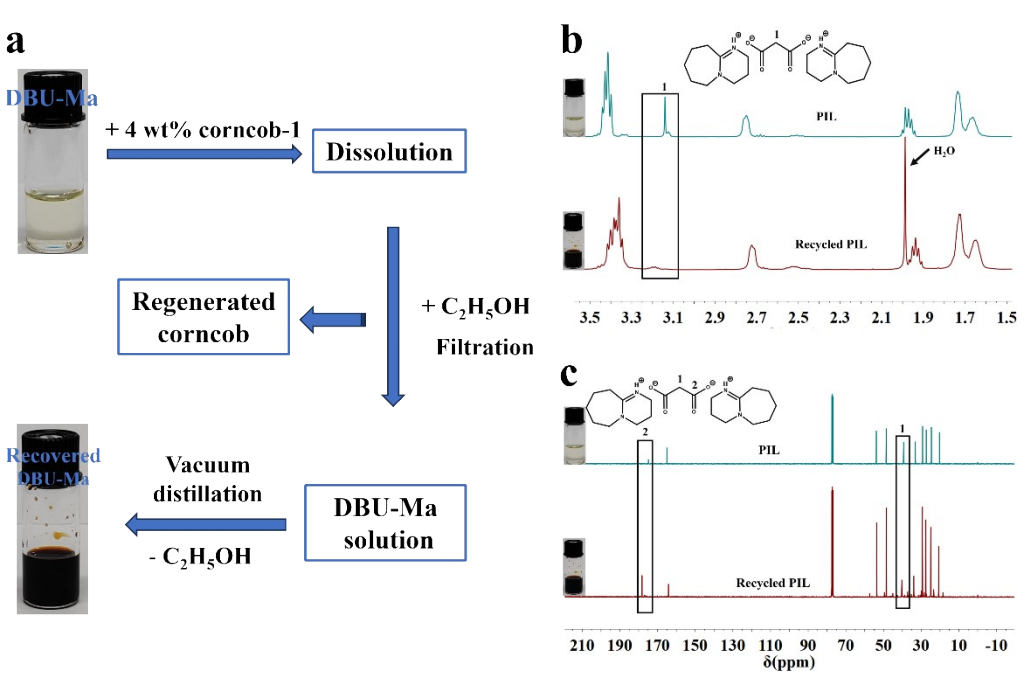

Figure S12. The recovery scheme for malonic acid-DBU PIL (a), ^{1}H (b), and ^{13}C (c) NMR of fresh malonic acid-DBU PIL and recovered malonic acid-DBU PIL.

In order to demonstrate the recovery potential of the solvent, the recovery of malonic acid-DBU PIL was investigated using the dissolution of corncob-1 as a template. The recovery scheme is shown in Figure S12a. First, 4 wt% corncob-1 was dissolved in malonic acid-DBU PIL. Then, an appropriate amount of anhydrous ethanol was added to the solution for stirring to obtain the regenerated corncob. The filtrate was obtained by filtration and the anhydrous ethanol was removed by distillation under reduced pressure to obtain recovered PIL. Finally, the dissolution of corncob-1 was continued using the recovered PIL to obtain a solubility of 1.2 wt%. ^{1}H and ^{13}C NMR spectra of fresh and recovered PIL were analyzed as shown in Figure 12b and c. It was evident in the ^{1}H NMR spectra that the DBU signals were not significantly altered in the recovered PIL compared to the fresh PIL. However, the recovered PIL had a significantly weaker signal at position 1 of the malonic acid as well as the presence of a water signal. The presence of water hindered the disruption of the hydrogen bonding network by the anions and cations in the system, which weakened the dissolution of biomass[1]. ^{13}C NMR spectra also demonstrated the structural disruption of malonic acid, with different shifts in the signals at positions 1 and 2 of malonic acid in the recovered PIL. Moreover, it was evident from both ^{1}H and ^{13}C NMR spectra that some impurities appeared in the recovered PIL. In summary, the above factors led to a decrease in the dissolving capacity of the recovered PIL.

1. L. Zhang, B. X. Zhan, Y. P. He, Y. Q. Deng, H. Y. Ji, S. Peng and L. F. Yan, *Green Chemistry*, 2024, **26**, 8794-8807.
2. J. H. Chen, Q. Q. Xu, F. He, W. Yue, G. Hu, J. Y. Gan and H. B. Xie, *Acs Sustain Chem Eng*, 2022, **10**, 7134-7148.
3. Y. Wang, H. Wang, L. Chen, W. T. Wang, Z. H. Yang, Z. M. Xue and T. C. Mu, *Green Chemistry*, 2023, **25**, 4685-4695.